Using Gravitational Lens Geometry to Measure Cosmological Parameters

by

Susan E. Dorsher

Submitted to the Department of Physics
in partial fulfillment of the requirements for the degree of

BACHELOR OF SCIENCE

at the

MASSACHUSETTS INSTITUTE OF TECHNOLOGY

June 2004

Author .....
Department of Physics
May 18, 2004

Certified by .....
Professor Jacqueline N. Hewitt
Thesis Supervisor, Department of Physics
Thesis Supervisor

Accepted by .....
Professor David E. Pritchard
Senior Thesis Coordinator, Department of Physics

Using Gravitational Lens Geometry to Measure Cosmological Parameters

by

Susan E. Dorsher

Submitted to the Department of Physics
on May 18, 2004, in partial fulfillment of the
requirements for the degree of
BACHELOR OF SCIENCE

Abstract

We develop a technique for measuring cosmological parameters (Ω_M and w) using gravitational lens geometry, source and lens redshifts, and the velocity dispersion of the lensing galaxy. This technique makes use of the relation $\theta_E = 4\pi\frac{\sigma_v^2}{c^2}\frac{D_{LS}}{D_S}$, where the critical radius θ_E and the one-dimensional velocity dispersion of the lensing galaxy σ_v are observable and the angular diameter distance ratio D_{LS}/D_S is related to the source and lens redshifts z_{source} and z_{lens} through the cosmological model. We assess the feasibility of this technique by examining the dependence of that ratio on cosmological parameters, doing a Monte Carlo simulation with a singular isothermal sphere lens galaxy, and estimating the error due to the asymmetry of real lenses. We conclude that the method is feasible with a large lens sample and a nearly circular projected mass distribution. We expect errors of less than 0.1 in Ω_M for a flat universe with a cosmological constant and a lens sample selected so that the axial ratio $f > 0.8$ for each lens.

Thesis Supervisor: Professor Jacqueline N. Hewitt
Title: Thesis Supervisor, Department of Physics

Acknowledgments

I would like to thank Professor Jacqueline Hewitt for her guidance over the course of this project and for funding the early stages of my work.

Contents

List of Figures

List of Tables

Chapter 1

Introduction

1.1 Gravitational Lensing

Gravitational lensing, or the deflection of light by massive objects, provides one of the most stunning tests of Einstein's theory of general relativity. Qualitatively, Newtonian physics and general relativity are in agreement, but general relativity predicts that light will be deflected around massive bodies by an amount twice as large as that predicted by Newtonian physics. In the total solar eclipse of 1919, measurements of the angular shift of stars near the sun confirmed Einstein's predictions.

In some cases, light may follow multiple paths around a lensing object to reach the observer, producing multiple images of the source. The separation between such images increases as the mass of the lensing object increases. In general, stars produce image separations that cannot be resolved by current technology. This effect may still be seen in two forms. Galaxies may lens more distant galaxies, resulting in observable image separations. These systems are useful in studying both galactic dynamics and the evolution of the universe. In cases where separate images cannot be resolved, micro-lensing, or the temporary brightening of the object, may be observed. This effect is due to changes in the solid angle subtended by the image induced by lensing, though the surface brightness of the source object remains constant. Micro-lensing is useful as a technique for locating compact dark objects in the halo of the Galaxy, a candidate for dark matter.[2]

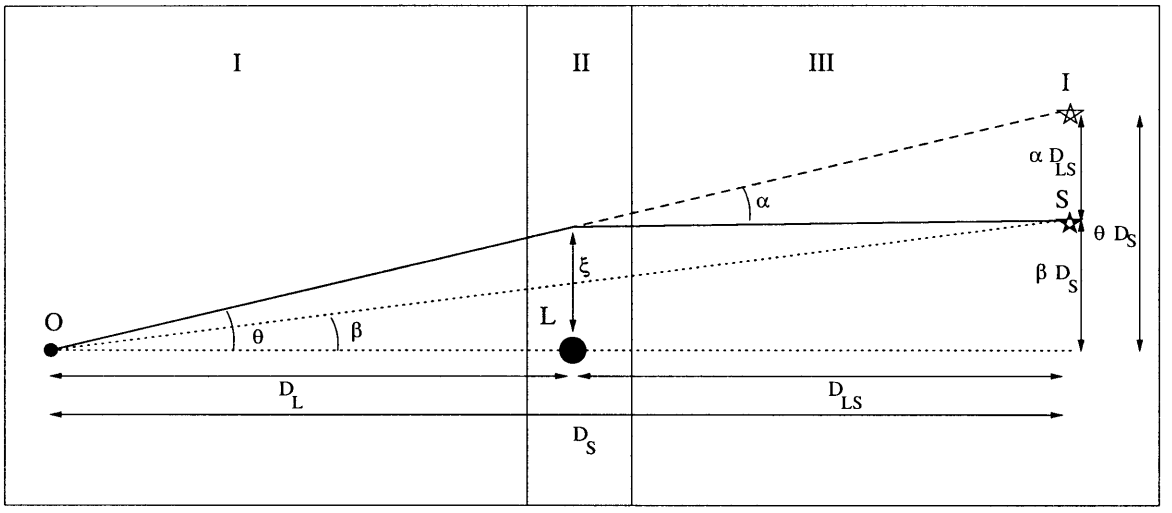

Figure 1-1: Gravitational lens system geometry. This figure depicts only one possible path for light, which may sometimes go around the other side of the lens or follow a path that comes out of the page, as well. O, L, S, and I represent the observer, lens, source, and apparent image position, respectively. Light follows the path of the solid line, from S to O. Other quantities shown are defined in the text.

Although precise calculations of light's path through curved space may be complex, the properties of gravitational lens systems are relatively easy to calculate because of several simplifying assumptions. Most of the deflection occurs within a small area about the lens, so the path may be broken into three segments, as in Figure 1-1. Before and after the lens (regions III and I), light travels through homogeneous space described by the Friedman-Lemaitre-Robertson-Walker metric. Any inhomogeneities can be treated as local perturbations, and introduced as either a second lens or shear. Around the lens system (region II), the scale is small enough the curvature of the universe as a whole is irrelevant; thus, we may assume space time is locally flat with a weak perturbation by the Newtonian potential Φ of the lensing object. This approximation is valid as long as $|\Phi| \ll c^2$ and the peculiar velocity of the lens is small compared to the speed of light.[2]

The deflection can be calculated from equations derived from the Schwarzschild metric in General Relativity. In this potential, photons move according to[34]

$$\frac{1}{b^2} = \frac{1}{L^2}\left(\frac{dr}{d\lambda}\right) + \frac{1}{r^2}\left(1 - \frac{2GM}{c^2 r}\right) \tag{1.1}$$

where the impact parameter $b = L/E$ is approximately equal to ξ in Figure 1-1, L is the angular momentum of the light about the lens, E is the energy of the photon, r is the distance of the photon from the lens, and λ is a parameter characterizing the path of the photon. By definition, $L = r^2 \sin^2\theta \frac{d\phi}{d\lambda}$, where ϕ is the angle about the lens from the photon's position at its source to its current position. These can be combined to give[34]

$$\frac{d\phi}{dr} = \pm\frac{1}{r^2}\left[\frac{1}{b^2} - \frac{1}{r^2}\left(1 - \frac{2GM}{c^2 r}\right)\right]^{-1/2} \tag{1.2}$$

The angle swept by the light between the source and the observer (which are both effectively at infinite distance) is given by $\Delta\phi = \alpha + \pi$. This angle can be found by integrating the above equation from the minimum value of r to infinity (half the path), then multiplying by two. The minimum radius occurs where $\frac{d\phi}{dr} = 0$. First, substitute a new variable $w = b/r$. This gives[34]

$$\Delta\phi = 2\int_0^{w_{max}} dw \left[1 - w^2\left(1 - \frac{2GM}{c^2 b}w\right)\right]^{-1/2}. \tag{1.3}$$

With a bunch of algebra and an integral table, this yields $\Delta\phi \approx \pi + \frac{4GM}{c^2 b}$ for small $\frac{GM}{c^2 b}$, which gives $\alpha = \frac{4GM}{c^2 b}$ for point mass or a spherically symmetric mass with a radius less than the impact parameter.

For an extended mass distribution, the deflection occurs over a small enough distance along the path of the light that the mass distribution may be approximated by its two dimensional projection along the line of sight. This projected distribution is given by[2]

$$\Sigma(\vec{\xi}) = \int \rho(\vec{\xi}, z) dz$$

where $\vec{\xi}$ is the position with respect to the center of mass in the plane of the projection, z is the position along the line of sight relative to the plane of the projection, and $\rho(\vec{\xi}, z)$ is the three dimensional mass distribution. Light is deflected at position $\vec{\xi}$

by[2]

$$\alpha(\vec{\xi}) = \int \frac{(\vec{\xi} - \vec{\xi'})\Sigma(\vec{\xi'})}{\left|\vec{\xi} - \vec{\xi'}\right|^2} d^2\xi'$$

Knowing the deflection angle, we can calculate the angular separation of the lens and the deflected images from the geometry of Figure 1-1. In the figure, D_L, D_S, and D_{LS} are the angular diameter distances (defined in Section 2.2) from the observer to the lens, from the observer to the source, and from the lens to the source, respectively. In general, $D_L + D_{LS} \neq D_S$, but instead is dependent on the cosmology. θD_S, αD_{LS}, and βD_S are the distances between the lens and source, source and image, and lens and image, respectively, projected out to a distance D_S and perpendicular to the line of sight. As an artifact of the definition of angular diameter distance, these distances do add linearly. Hence, we get the lens equation:[16]

$$\theta D_S = \beta D_S + \alpha D_{LS} \tag{1.4}$$

We can see from the Figure 1-1 that $\xi = \theta D_L$ and we know from the previous analysis that $\alpha = \frac{4GM}{c^2\xi}$ for outside a spherically symmetric lens. Combining these, we get $\theta_\pm = \frac{1}{2}\left[\beta \pm (\beta^2 + 4\theta_E^2)^{1/2}\right]$, where $\theta_\pm$ are the angular separation of the images and the lens and $\theta_E = \sqrt{\frac{4GM}{c^2\xi}\left(\frac{D_{LS}}{D_S D_L}\right)}$ is known as the critical radius.[16] When $\beta = 0$, there is no preferred axis for the images so they form a ring around the lens at the critical radius. This is known as an Einstein ring. Systems with asymmetric lens mass distributions or those with external shear form three or more images, introducing more degrees of freedom to the lens equation.

1.2 Cosmology

Modeling the evolution of the universe as a whole is both interesting in its own right and useful. Not only does it uncover a fascinating story of our past and future, but such a model also provides opportunities to test fundamental physics. Additionally,

a model of the universe is necessary to understand the propagation of light from far away galaxies and to interpret the images we take of the sky.

Two important assumptions lie behind this model, spatial isotropy and homogeneity. The assumption of isotropy states that the universe looks approximately the same in any direction, or that the universe is invariant under rotation. Composition, density, curvature, and physical laws of the universe are uniform at a given distance from Earth and a constant moment in time, independent of the angle on the sky. Obviously, since we see stars, star clusters, galaxies, and clusters of galaxies, this is only approximately true. However, over a large enough scale the universe can be well approximated by an isotropic model. We see evidence of isotropy in the large scale distribution of galaxies. Measurements of the Cosmic Microwave Background (CMB), radiation left over from the early universe, tell us that the early universe was isotropic to better than one part in 1000.[16]

In a homogeneous universe, the universe looks the same at every point in space at a constant time. More mathematically, the universe is invariant under translation. The composition and densities are the same, the curvature is the same, and the physical laws are the same. This is of course not true on a small scale. Our galaxy has a density that is far from uniform and much greater than the density of the intergalactic medium. However, on a large enough scale, the universe should be approximately homogeneous. This expectation comes from the Copernican principle, which states that we are not the center of the universe.[16] Additionally, counts of galaxy density over medium sized volumes support the postulate of homogeneity, if the volume chosen is large enough to blur local fluctuations but small enough that galaxies do not evolve significantly in the time it takes for light to travel from one side to another.

We construct this model out of a metric derived from general relativity. Although isotropy and homogeneity demand that the universe be invariant under spatial rotations and translations, the metric may evolve arbitrarily with time. It is assumed that local fluctuations in density and curvature are small enough that they may be treated as perturbations to this highly symmetric metric. We use polar coordinates centered

at Earth to simplify calculations of physically measured quantities since light travels radially to us from stars and galaxies. However, homogeneity and isotropy together demand that these coordinates could be centered anywhere in the universe and the metric would hold. The most general metric satisfying these conditions is given by[7]

$$ds^2 = -dt^2 + a^2(t)\left[\frac{dr^2}{1-\kappa r^2} + r^2\left(d\theta^2 + sin^2\theta d\phi^2\right)\right] \tag{1.5}$$

where t is the time coordinate, r, θ, and ϕ are spatial coordinates, and $a(t)$ is an expression known as the scale factor that governs the time evolution of the distance between coordinate points. World lines that remain at constant spatial coordinates for increasing time are geodesics in this metric. Hence, a galaxy at coordinate distance r from Earth will remain at that coordinate distance for all time. The physical distance between the same two points will change like $a(t)r$.

This metric represents three different curvatures depending on the value of κ. The curvature of the metric can be described using only $\kappa = 0, 1, -1$, since the magnitude of curvature can be subsumed into the choice of coordinates. These three values of κ correspond to flat, closed, and open universes respectively. A flat universe corresponds to Euclidean geometry, with parallel lines that never meet and triangles that contain 180 degrees. The closed universe is just $S_{(3)}$, which can be described as a a three-sphere embedded in four-dimensional space.[7] It has finite volume, parallel lines cross twice, a long enough straight line will form a closed loop, and triangles have more than 180 degrees. The open universe is somewhat harder to visualize. Embedded in four dimensions, it is the three dimensional equivalent of a saddle. Its volume is infinite, parallel lines diverge, and triangles have less than 190 degrees.

Recent measurements of the cosmic microwave background (CMB) suggest that our universe is flat or very close to it.[16] This background radiation comes from the blackbody radiation emitted by the soup of particles in the early universe. When the universe was hot enough, electrons were not yet bound into atoms. During this time photons could not travel a significant distance without being scattered or re-absorbed.

The first light we see from the distant (and early) universe occurs at an era known as Recombination, when the electrons settled into atoms and the universe became transparent. This light has been gravitationally red-shifted to about a thousandth of its original frequency and now forms the CMB. The curvature of the universe can be measured by looking at the angle scale of anisotropies in this radiation. The length scale of these anisotropies should be set by the distance sound could travel in the era prior to recombination, something that is believed to be well-known. The curvature of the universe determines the relationship between a length at a given distance and the angle on the sky, hence these anisotropies provide a test of the curvature of the universe. The recent WMAP results agree with a flat universe to within two percent.[16] Because this result is expected in light of inflationary theory and because the agreement is so good, in this paper we will assume the universe is flat.

We calculate the scale factor by combining the Friedman equation, the first law of thermodynamics, and the equations of state of various components in the universe. The Friedman equation comes from the t,t component of the Einstein equation for a perfect fluid in a Robertson-Walker metric. The equation is given by[16]

$$\dot{a}^2 + k = \frac{8\pi\rho(t)}{3}a^2 \tag{1.6}$$

where $\dot{a}$ is the time derivative of the scale factor, k is the curvature, and $\rho(t)$ is the total energy density of the universe as a function of time. This equation can also be derived from Newtonian gravity, where it may be interpreted as the equation relating kinetic and potential energy.

For the cosmological fluid, the first law of thermodynamics states that if a volume V contracts infinitesimally, the total energy $E = \rho V$ is changed by $dE = -pdV$, where ρ is the energy density and p is the pressure of the fluid.[16] The volume can be rewritten in terms of the scale factor and the coordinate volume: $V = a^3(t)V_{coord}$. Dividing by dt and factoring out the coordinate volume, which is time-independent,

yields[16]

$$\frac{d}{dt}\left[\rho(t)a^3(t)\right] = -p(t)\frac{d}{dt}\left[a^3(t)\right] \tag{1.7}$$

These two equations, together with the equations of state for each separate component of the cosmological fluid, can be used to derive the time evolution of the scale factor. To the best of our knowledge, the cosmological fluid is made of three different kinds of components, each with a different equation of state. Baryonic matter (such as protons or electrons) is pressureless, yielding an energy density proportional to $1/a^3(t)$. Photons (and other massless particles like neutrinos) obey $p = \frac{1}{3}\rho$ and evolve according to $\rho \propto 1/a^4(t)$. A third kind of fluid, known as dark energy, will be discussed in the following section. We divide these energy densities by the critical density, $\rho_{crit} = \frac{3H_0^2}{8\pi}$, where $H_0 = \dot{a}(t_0)/a(t_0)$ and t_0 is the present time. This results in dimensionless quantities Ω_M, Ω_r, and Ω_Λ corresponding to matter, radiation, and vacuum energy fractions, respectively.[33] In a flat universe, these fractions sum to one. We can show both empirically and theoretically that radiation dominated the early universe, while baryonic matter and dark energy dominate the universe today, yielding (approximately) $\Omega_m + \Omega_\Lambda = 1$ in the present-day universe. In a flat universe with only baryonic matter ($\Omega_m = 1$), the scale factor evolves like $a(t) = (t/t_0)^{2/3}$.[16]

Once we know the evolution of the scale factor, we can calculate how light propagates through the universe. Radial lines are geodesics, so in the absence of local perturbations, the only interesting effect is the change in frequency. Light travels with zero proper time ($ds = 0$) and radial paths have $d\theta = d\phi = 0$. Thus, the metric yields $dr = \frac{dt}{a(t)}$ for light emitted at $r = R$ at $t = t_e$ and observed at $r = 0$ at $t = t_o$. By integrating both sides, we can relate the distance light travels to its times of emission and observation. We obtain $R = \int_{t_e}^{t_o} \frac{dt}{a(t)}$.[16]

Now we consider light pulses emitted with a frequency of $\omega_e = \frac{2\pi}{\delta t_e}$, where δt_e is the time separation between pulses at emission. We define ω_o and δt_o similarly. Successive pulses travel the same spatial separation R between emission and observation, so $\int_{t_e+\delta t_e}^{t_o+\delta t_o} \frac{dt}{a(t)} = \int_{t_e}^{t_o} \frac{dt}{a(t)}$. Because these integrals differ only by an infinitesimal amount

on either end and must be equal for all $a(t)$, we know $\frac{\delta t_e}{a(t_e)} = \frac{\delta t_o}{a(t_o)}$. From this, we can write $\frac{\omega_o}{\omega_e} = \frac{a(t_e)}{a(t_o)} = 1 + z$, where z is the redshift, defined such that $1 + z = \frac{\omega_o}{\omega_e}$. Thus, for any increasing $a(t)$, light frequency is reduced from time of emission at time of observation.[16]

This reduced frequency is known as cosmological redshift. In 1929, Hubble observed that galaxies followed the approximate relation of $z = H_0 d$, where z is the redshift, H_0 is the Hubble constant, and d is the distance obtained from parallax or from magnitude measurements of objects with known luminosity. Hubble assumed the redshift was due to Doppler shifts from the recession velocity of these galaxies. Thus, his famous relation $v = H_0 d$, where v is the recession velocity of the galaxy.

1.3 Dark Energy

Dark energy is a discovery of the last decade. Prior to that, models of the universe assumed that the entire energy density was due to baryonic matter. In the late 1990s, several different surprising experimental results forced us to alter our models. Better measurements of the matter density showed convincingly that $\Omega_M = 0.3 \pm 0.1$. At the same time, CMB measurements indicated that the universe must be within a couple percent of flat. This combination required that some kind of substance, dubbed dark energy, make up the difference between the critical density for a flat universe and the observed matter density. Observations of type Ia supernovas as standard candles to measure distance to receding galaxies determined that the expansion of the universe is accelerating, a fact that can only be explained by some kind of negative pressure in the universe. A substance with negative pressure that explains these results also would account for the difference between the critical density and the matter density; thus, we learned that dark energy must have a negative pressure.[33]

There are several different ways to model dark energy. The two most common formulations are the cosmological constant and quintessence. For a cosmological constant, the energy density remains fixed in time and does not vary with the scale factor. This corresponds to a vacuum energy, where the energy belongs to space itself.

The equation of state of dark energy is $p_\Lambda = -\rho_\Lambda$ and the cosmological constant is given by $\Omega_\Lambda = \rho_\Lambda/\rho_{crit}$ evaluated at the present time. A universe with both a cosmological constant and a matter density no longer has an analytical solution $a(t)$ to the Freedman equation, though it remains possible to calculate a numerical solution for given cosmological parameters.[16]

The alternative to a cosmological constant is quintessence. This theory states that a scalar field pervades the universe and changes in time, producing the negative pressure and the energy density of dark energy. This scalar field would be similar to though weaker than the one responsible for inflation. Several different mathematical models are possible for such a field, though all allow values of w other than negative one in the equation of state $p = w\rho$. The energy density $\rho \propto a^{-3(1+w)}$ for these fields.

Neither quintessence nor a cosmological constant is predicted by prior theories. Current measurements constrain w very little so both possibilities remain wide open. The nature of dark energy is truly a mystery.

1.4 Constraining Cosmological Parameters

Supernova and CMB data together provide our current best estimates of cosmological parameters, $\Omega_M = 0.3 \pm 0.1$ and $\Omega_\Lambda = 0.7 \pm 0.1$[7]. These measurements have been checked by multiple observations, but another independent method would be useful both to narrow the available range of parameters and to provide a check in case one or both of these experiments suffers from unnoticed systematic errors.

Gravitational lensing geometry, combined with lens mass, provides a measure of angular diameter distances. Angular diameter distances are related to the cosmological model, and through that to the redshift. Thus, redshifts of source and lens galaxies in high redshift gravitational lens systems could be combined with lens geometry and some measure of lens mass to give another independent measure of cosmological parameters.

Chapter 2

Proposed Experiment

2.1 Measuring Lens Mass

As a first approximation, for developing and analyzing the potential of this method, we will use a singular isothermal spheres (SIS) model of lens mass distribution. Light passing around or through this spherically symmetric mass distribution obeys the lens equation derived in Section 1.1. In this model, we assume the lensing galaxy consists of an ideal gas of stars (which we treat as particles) at a single, constant temperature. The ideal gas law says $pV = NkT$, where p is the pressure, V is the volume, N is the total number of stars, k is Boltzmann's constant, and T is the temperature. Since the density $\rho = mN/V$, where m is the mass of a star, $p = \frac{\rho kT}{m}$.

The one dimensional velocity dispersion σ_v is defined such that $m\sigma_v^2 = kT$, so a particle moving with a velocity equal to σ_v has a kinetic energy equal to the mean energy of a star in the system.[2] The velocity dispersion can be measured from the width of spectral lines emitted by stars in the lensing galaxy. Some random velocities of stars will be oriented toward Earth, increasing the frequencies of the spectral lines, and some will be oriented away from us, decreasing the frequencies. Since the galaxy appears as a point in the sky, the spectral lines will sum into a single, wide spectral line with a width related to the velocity distribution of stars in the galaxy and hence to the velocity dispersion. From this definition and the ideal gas law, we can write $p = \rho\sigma_v^2$.

In order to maintain hydrostatic equilibrium, the gravitational force inward on the stars must balance the force outward due to the pressure gradient. This yields the equation of hydrostatic equilibrium,[2]

$$\frac{dp}{dr} = -\frac{GM(r)\rho}{r^2}, \frac{dM}{dr} = 4\pi r^2 \rho \tag{2.1}$$

where r is the radial distance from the center of the galaxy and $M(r)$ is the total mass interior to r. The second equation above is merely combines the definition of density with the volume element for radial integration. From the two equations above and $p = \rho\sigma_v^2$, we can find $\rho(r) = \frac{\sigma_v^2}{2\pi G}\frac{1}{r^2}$ and $M(r) = \frac{2\sigma_v^2 r}{G}$. This model is unphysical both because the density is infinite at $r = 0$ (the singular part of the SIS model) and because the mass increases to infinity with infinite distance. However, it is useful as a first approximation and can successfully replicate some physical features of galaxies.[2]

From this mass distribution, we can calculate the lensing geometry. Equations developed in Section 1.1 allow us to project the mass distribution to two dimensions then determine the deflection angle from that projected distribution. We find a projected mass distribution of $\Sigma(\xi) = \frac{\sigma_v^2}{2G}\frac{1}{\xi}$. The deflection angle is then $\alpha = 4\pi\frac{\sigma_v^2}{c^2}$. Plugging this into the lens equation with $\beta = 0$ and solving for θ yields a critical radius of[2]

$$\theta_E = 4\pi\frac{\sigma_v^2}{c^2}\frac{D_{LS}}{D_S} \tag{2.2}$$

Of the variables in the above equation, θ_E and σ_v^2 are directly observable. This means we can directly measure the ratio $\frac{D_S}{D_{LS}} = 4\pi\frac{\sigma_v^2}{\theta_E c^2}$. This ratio can also be related to the redshifts of the source and lens galaxies through the cosmological model. The relation of these redshifts to this ratio allows us to constrain cosmological parameters.

2.2 Relating Redshift to Angular Diameter Distance

The angular diameter distance is defined to be the ratio of an object's transverse length to the angle it subtends, in radians. The relation of angular diameter distance to redshift depends on the curvature. This relation is given by the following equations [17]

$$D = \begin{cases} \frac{c}{H_0\sqrt{\Omega_k}(1+z)} \sinh\left[\sqrt{\Omega_k}\int_0^z \frac{dz'}{E(z')}\right] & \text{for } \Omega_k > 0 \\ \frac{c}{H_0(1+z)}\int_0^z \frac{dz'}{E(z')} & \text{for } \Omega_k = 0 \\ \frac{c}{H_0\sqrt{|\Omega_k|}(1+z)} \sin\left[\sqrt{|\Omega_k|}\int_0^z \frac{dz'}{E(z')}\right] & \text{for } \Omega_k < 0 \end{cases} \tag{2.3}$$

where D is the angular diameter distance, z is the redshift, and

$$E(z) = \sqrt{\Omega_M(1+z)^3 + \Omega_k(1+z)^2 + \Omega_\Lambda(1+z)^{3(1+w)}}. \tag{2.4}$$

In the previous equation, w comes from the equation of state $p = w\rho$. For a cosmological constant, $w = -1$ and $3(1+w) = 0$.

Angular diameter distances do not add linearly. The angular diameter distance D_{12} between objects located along the same line of sight at D_1 (corresponding to z_1) and D_2 (corresponding to z_2) is not $D_2 - D_1$. For a flat universe ($\Omega_k = 0$), $D_{12} = \frac{1}{1+z_2}[(1+z_2)D_2 - (1+z_1)D_1]$ [17]. With this equation, we can now relate the ratio $\frac{D_{LS}}{D_S}$ to the (observable) redshifts of the source and the lens galaxies through the cosmological parameters. Most interestingly, we learn that although calculating angular diameter distances from redshifts requires knowledge of the Hubble constant (H_0), a ratio of these distances is independent of H_0. Thus, such a ratio may allow more sensitive measurements of matter density or the cosmological constant and its evolution because the poorly-known Hubble constant is eliminated from the relation.

2.3 Distance Ratio as a Function of Cosmological Model

We have seen that we can directly measure the ratio $\frac{D_S}{D_{LS}} = 4\pi\frac{\sigma_v^2}{\theta_E c^2}$, which we may then relate to cosmological parameters using the redshifts of the source and lens galaxies. The usefulness of this ratio as a measure of cosmological parameters depends on how sensitive it is to changes in those parameters. To answer that question we plot the ratio $\frac{D_S}{D_{LS}}$ for various combinations of source and lens redshifts as a function of those cosmological parameters. Figure 2-1 shows the relationship between lens redshift and this ratio of angular diameter distances for a source redshift of 3.0 for various flat cosmological models with a cosmological constant. Figure 2-2 plots this distance ratio against the matter density for a particular lens system in a flat universe with a cosmological constant. Figure 2-3 plots D_S/D_{LS} against w for the same lens system in a flat universe $\Omega_M = 0.3$.

The value of D_S/D_{LS} is dependent on both σ_v and θ_E, but the error will be dominated by σ_v. Velocity dispersions can be measured to approximately 5 percent accuracy with current technology. Thus, since $D_S/D_{LS} \propto \sigma_v^2$, we expect a 10 percent error on D_S/D_{LS}. If we assume currently accepted values of $\Omega_M = 0.3$ and $w = -1$ are approximately right, we can produce a crude estimate of errors on Ω_M and w determined from this ratio of angular diameter distances (see Figures 2-2 and 2-3). We expect to be able to constrain $0.12 < \Omega_M < 0.65$ and $-6 < w < -0.2$. These are not promising results, particularly for w. However, a slight improvement in measurement techniques would result in a dramatic improvement in constraints on Ω_M because of the flat slope of the curve at large Ω_M. Because of this sensitivity, it is worth examining the feasibility of this method in greater detail to obtain a less crude estimate of potential error bars.

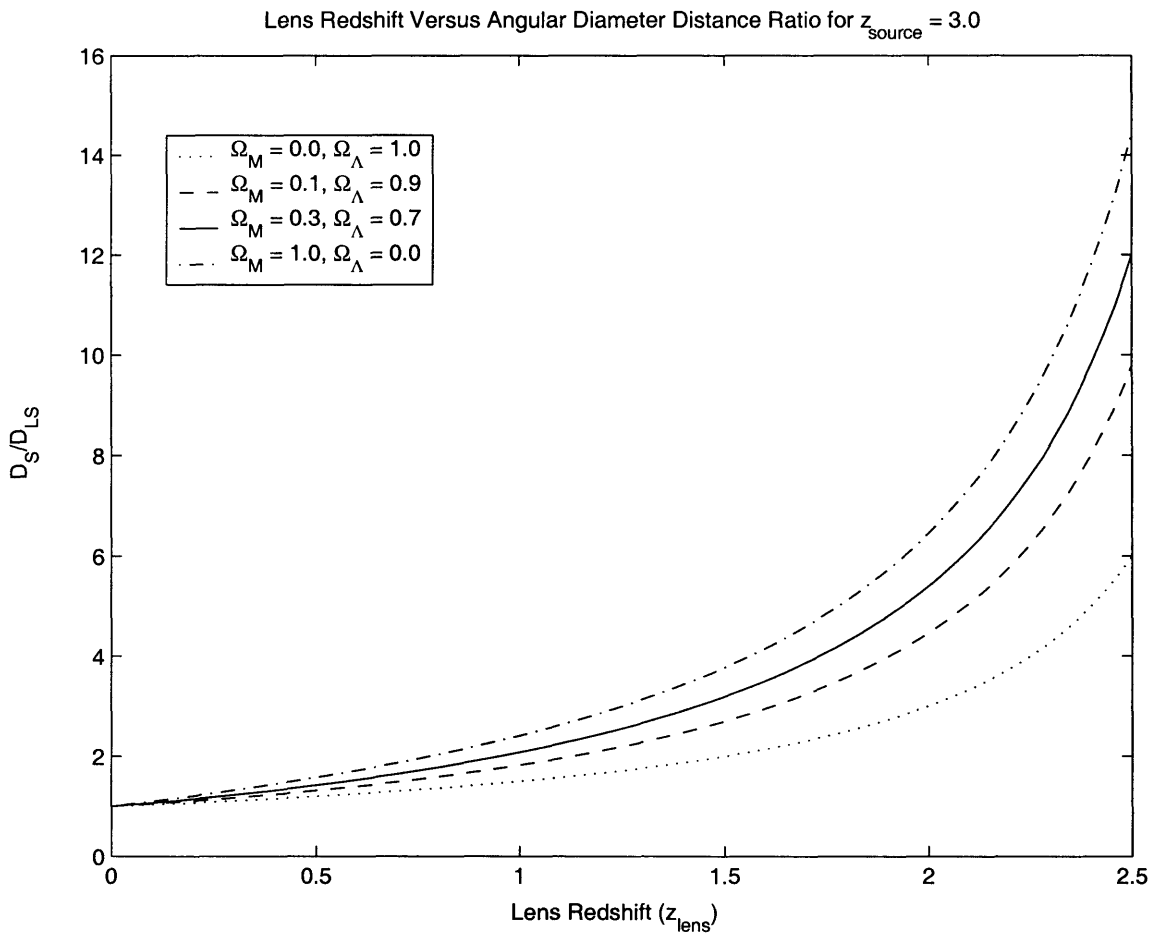

Figure 2-1: The ratio of angular diameter distances versus lens redshift for various flat models of the universe with a cosmological constant. These plots assume $z_{source} = 3.0$.

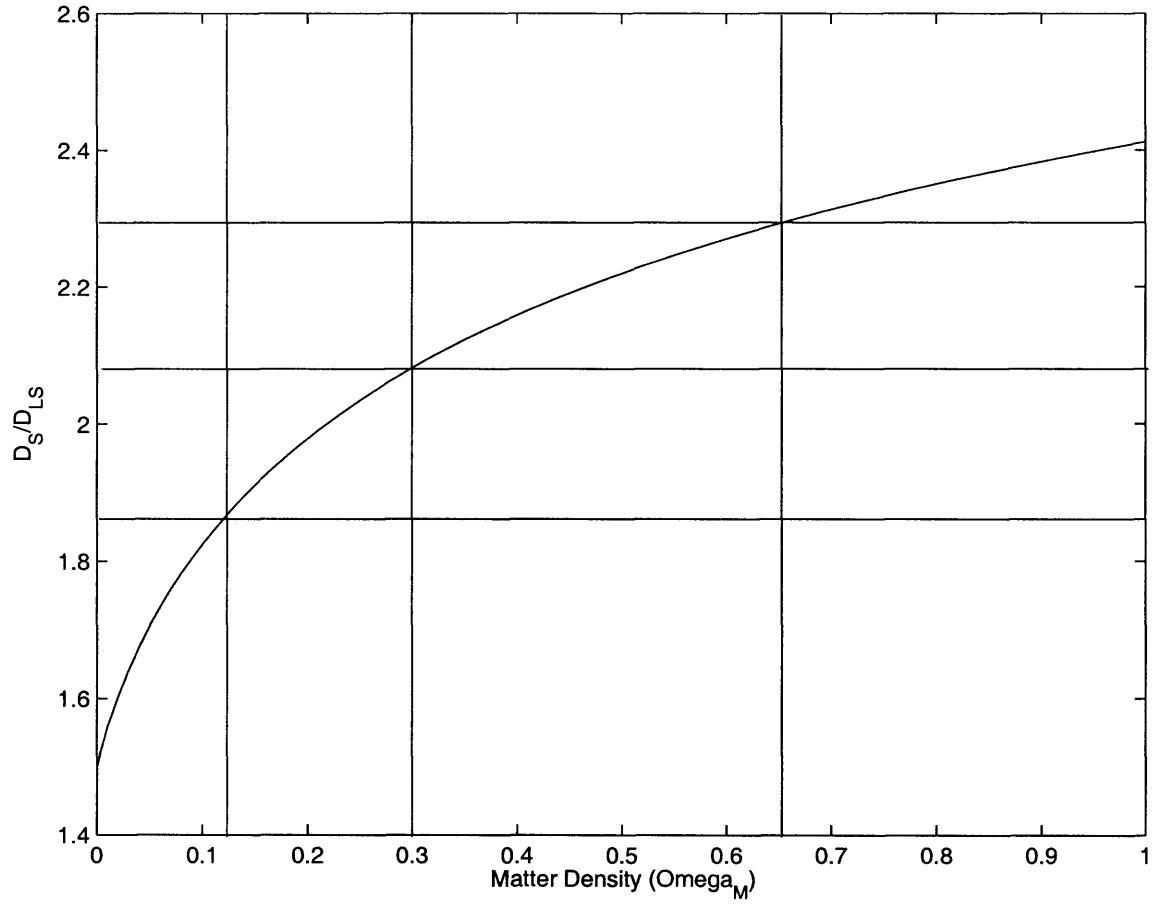

Figure 2-2: The ratio of angular diameter distances versus the matter density of the universe in a flat universe with a cosmological constant. This plot is for a lens system with $z_{source} = 3.0$ and $z_{lens} = 1.0$. The middle horizontal and vertical lines show the expected value of $\Omega_M = 0.3$ and its corresponding expected value of D_S/D_{LS}. The outer horizontal and vertical lines form a box corresponding to a 10 percent error in D_S/D_{LS} for that expected value.

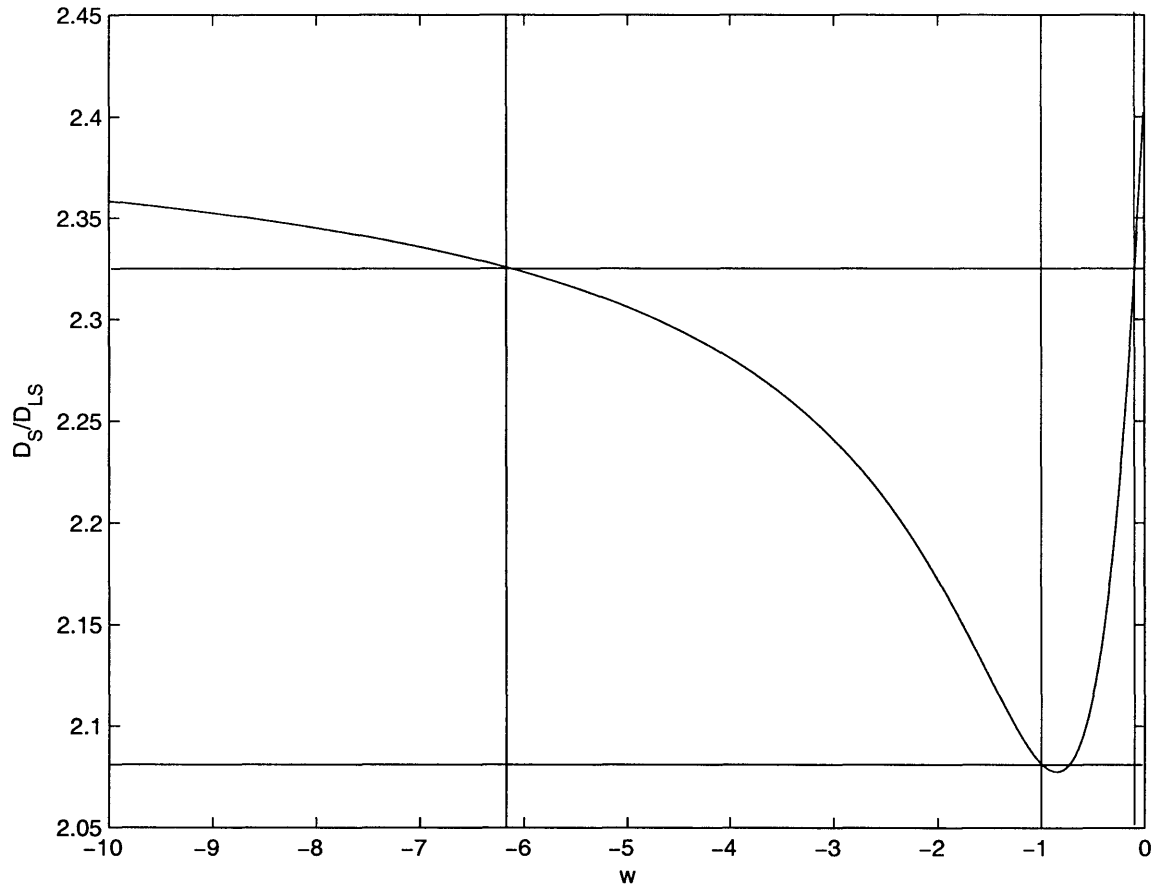

Figure 2-3: The ratio of angular diameter distances versus w for a a flat universe with $\Omega_M = 0.3$ and $\Omega_\Lambda = 0.7$. This plot is for a lens system with $z_{source} = 3.0$ and $z_{lens} = 1.0$. The middle vertical line and lower horizontal line show the expected value of $w = -1.0$ and its corresponding D_S/D_{LS}. The upper horizontal line and the outer two vertical lines bound the region of 10 percent error on $D_S/_{LS}$ for this expected w.

2.4 Proposed Measurement

We propose that the matter density of the universe may be measured using a sample of gravitational lens systems with known source and lens redshifts, critical radius, and lensing galaxy one-dimensional velocity dispersions. We assume the validity of the CMB results and hence a flat universe in our calculations. The ratio of two angular diameter distances, D_S/D_{LS}, can be related to the critical radius and velocity-dispersion through the following equation:

$$\frac{D_S}{D_{LS}} = 4\pi\frac{\sigma_v^2}{\theta_E c^2}. \tag{2.5}$$

We can also relate this ratio to the galaxy redshifts and the cosmological model using the $\Omega_k = 0$ version of the equations in Section 2.2. Thus, we propose measuring z_{source}, z_{lens}, σ_v, and θ_E for each system. From this sample, best fit values of Ω_M and w may be obtained by maximizing the likelihood function for the sample and the general cosmological model of a flat universe with no radiation. Because all measured values are independent, this corresponds to minimizing the χ^2, given by

$$\chi^2 = \sum_i \frac{\left(\sigma_{calculated,i} - \sigma_{v,i}\right)^2}{\sigma^2_{\sigma_{v,i}}} \tag{2.6}$$

where i is the index labelling the lens systems, $\sigma_{v,i}$ is the velocity dispersion of the ith system. In the preceding equation, $\sigma^2_{\sigma_{v,i}}$ is the variance of the velocity dispersions of the sample, and

$$\sigma_{calculated,i} = \sqrt{\frac{\theta_{E,i}c^2}{4\pi}\frac{D_S\left(z_{source,i}, \Omega_M, w\right)}{D_{LS}\left(z_{lens,i}, z_{source,i}, \Omega_M, w\right)}} \tag{2.7}$$

where $\theta_{E,i}$ is the critical radius of the ith system, D_S is the angular diameter distance from the observer to the ith source as a function of measured and varied parameters, D_{LS} is the angular diameter distance from the ith lens to the ith source as a function of measured and varied parameters, $z_{source,i}$ is the redshift of the ith source, and $z_{lens,i}$ is the redshift of the ith lens.

Chapter 3

Simulated Measurement with Singular Isothermal Sphere Lenses

The feasibility of the technique described in the previous chapter may be examined using a simulated set of data, analyzed in the manner of real data. In this chapter, we will examine this technique if data is interpreted with the assumption that lensing galaxies may be modeled as singular isothermal spheres. This assumption is clearly false but provides a starting point for the feasibility assessment. The next chapter will examine the effect of introducing asymmetries in the lensing galaxy.

3.1 Lens Sample

To assess the feasibility of this technique for measuring cosmological parameters, we must find a way to estimate the error associated with this measurement for each cosmological parameter. This will require some idea of what results we expect from our measurements. We will use lens systems with previously measured redshifts and critical radii to create a sample set of expected results, which we will use as a basis for our feasibility analysis. We limit our lens sample to systems with four images or an Einstein ring. In such systems, the critical radius is particularly well constrained. Precise determination of the critical radius is important to the success of this observational technique. These constraints applied to the body of measurements

Table 3.1: Gravitational lens system data used in the Monte Carlo simulation. These numbers correspond to previous measurements of the system, except as marked. This list consists of all lens systems with a known source redshift and either 4 images or an Einstein ring at the time the list was compiled (September 2002). For systems marked with [1], z_{lens} is unknown. The listed number (used in the simulation) corresponds to half the source redshift or one, whichever is less. This is a reasonable approximation of the likeliest position of the lens galaxy, statistically. For systems marked with [2], the critical radius has not been measured. This value (used in the simulation) corresponds to half the maximum image separation.

Lens System	z_{source}	z_{lens}	θ_E	Type of Lens System	References
0047-2808	3.595	0.485	1.35	4 image	[11],[38],[39]
0218+357	0.94	0.686	0.33[2]	2 image and Einstein ring	[11],[29],[40],[5]
0230-2130	2.16	1.0[1]	1.1[2]	4 image	[11],[41]
0414+0534	2.639	0.468	1.15	4 image	[11],[24],[12],[36],[3]
0712+472	1.339	0.4060	0.64[2]	4 image	[11],[14]
0751+2716	3.200	0.3502	0.4	Einstein ring	[11],[37]
0810+2554	1.5	0.75[1]	0.5[2]	4 image	[11],[32]
0911+0551	2.8	0.78	1.55[2]	4 image	[11],[6]
1115+080	1.722	0.311	1.1	4 image	[11],[42],[22],[19]
14113+5211	2.811	0.465	1.14	4 image	[11],[26]
1413+117	2.55	1.0[1]	0.68[2]	4 image	[11],[8]
14176+5226	3.394	0.81	1.51	4 image	[11],[31],[10]
1422+231	3.62	0.64	0.65[2]	4 image	[11],[30],[21],[1]
1555+375	1.59	0.42	0.21[2]	4 image	[11]
1608+656	1.394	0.6304	1.04[2]	4 image	[11],[28],[13]
1654+1346	1.74	0.254	1.05[2]	Einstein ring	[11],[23],[20]
1830-211	2.507	0.886	0.49[2]	2 image and Einstein ring	[11],[15],[27],[25]
2045+265	1.28	0.87	0.93[2]	4 image	[11],[18]
2237+030	1.69	0.04	1.76	4 image	[11]

available in September 2002 yield the results in Table 3.1, which contains the data we used to model our proposed measurement.

3.2 Precision of Measurements

We will also have to assume something about the precision of the measurements we could make to assess the feasibility of this technique. As in Section 2.3, we will assume that velocity dispersion measurements dominate the error and neglect error due to other measurements. We neglect errors in lens redshifts, source redshifts, and

critical radii, which are expected to be much smaller than the errors in the velocity dispersions. Our simulated measurement will assume 5% errors in σ_v that can be modeled with a Gaussian probability distribution. In other words, we will assume that each measurement of σ_v is equal to its true value plus a random error picked from a Gaussian distribution with the square root of the variance equal to five percent of the true velocity dispersion.

3.3 The Cosmos

Finally, we must assume a true model of the universe to predict the results of this measurement technique. Throughout our simulation we assume a flat universe with insignificant radiation density dominated by matter and a cosmological constant ($\Omega_{M,true} = 0.3$, $\Omega_{\Lambda,true} = 0.7$, $w_{true} = -1.0$). We obtain the errors on our (simulated) measured cosmological parameters by first constructing simulated observed values of σ_v by adding a five percent error to the predicted values for this cosmological model given our lens data and a SIS lens model. We then minimize the χ^2 for this simulated set of observational data to obtain our simulated observed values of cosmological parameters. Repeating this process a large number of times generates a probability distribution for each observed cosmological parameter whose width predicts the random observational error associated with this measurement technique.

3.4 Monte Carlo

Our Monte Carlo simulation, then, is produced by the following algorithm:

1. Assume a true universe of $\Omega_{M,true} = 0.3$, $\Omega_{\Lambda,true} = 0.7$, and $w_{true} = -1.0$. These values will not be the same as the values "measured" in the simulation, but rather represent an abstract, assumed truth about the universe.

2. Create a simulated set of observed data. We do this by:

(a) Assigning $z_{source,i}$, $z_{lens,i}$, and $\theta_{E,i}$ for each lens system (labelled by an index i) as shown in Table 3.1. We assume these values are perfectly accurate and precise.

(b) Calculating $D_{S,i}/D_{LS,i}$ for each lens assuming the true universe defined above and using $z_{source,i}$ and $z_{lens,i}$. We do this using the equations for a flat universe given in Section 2.2 that relate angular diameter distance to redshift.

(c) Calculating $\sigma_{v,true,i} = \sqrt{\frac{\theta_{E,i}c^2}{4\pi}\frac{D_{S,i}}{D_{LS,i}}}$ for each system. This value also does not correspond to any measurement, but represents the true velocity dispersion that a perfect measurement would obtain in this simulated universe. Furthermore, this prediction is only valid if lenses can be modeled as singular isothermal spheres, an assumption tested in the next chapter.

(d) Assigning the observed velocity dispersion σ_v to be $\sigma_v = \sigma_{v,true,i} + x$, where x is a random number drawn from a Gaussian probability density function given by $P(x) = \frac{1}{\sqrt{2\pi(0.05\sigma_{v,true,i})^2}} exp\left(-\frac{x^2}{2(0.05\sigma_{v,true,i})^2}\right)$. This is the only step that need be repeated to create a new set of observed data, since the others only depend on values that remain constant throughout the simulation.

3. Maximize the likelihood (or minimize the χ^2) of this data set by varying the measured cosmological parameters. Several different assumptions could go into the way the parameters are varied. They could all be varied at once, freely, or some could be held fixed. We favored a flat universe ($\Omega_\Lambda = 1 - \Omega_M$) with w fixed to $w = -1.0$, leaving only one independent parameter, because of the clarity of the CMB results and the inability of this method to measure w, as shown in the previous section.

   For a flat universe, $\chi^2 = \sum_i \frac{\left(\sigma_{v,predicted,i} - \sigma_{v,i}\right)^2}{\sigma^2_{\sigma_{v,i}}}$, where $\sigma^2_{\sigma_{v,i}}$ is the variance of the $\sigma_{v,i}$s and $\sigma_{v,predicted,i}$ is calculated by the same process as $\sigma_{v,true,i}$ but with varied cosmological parameters rather than the true cosmological parameters. The varied cosmological parameters that minimize χ^2 for a given simulated data set are the measured cosmological parameters for that data set. This step,

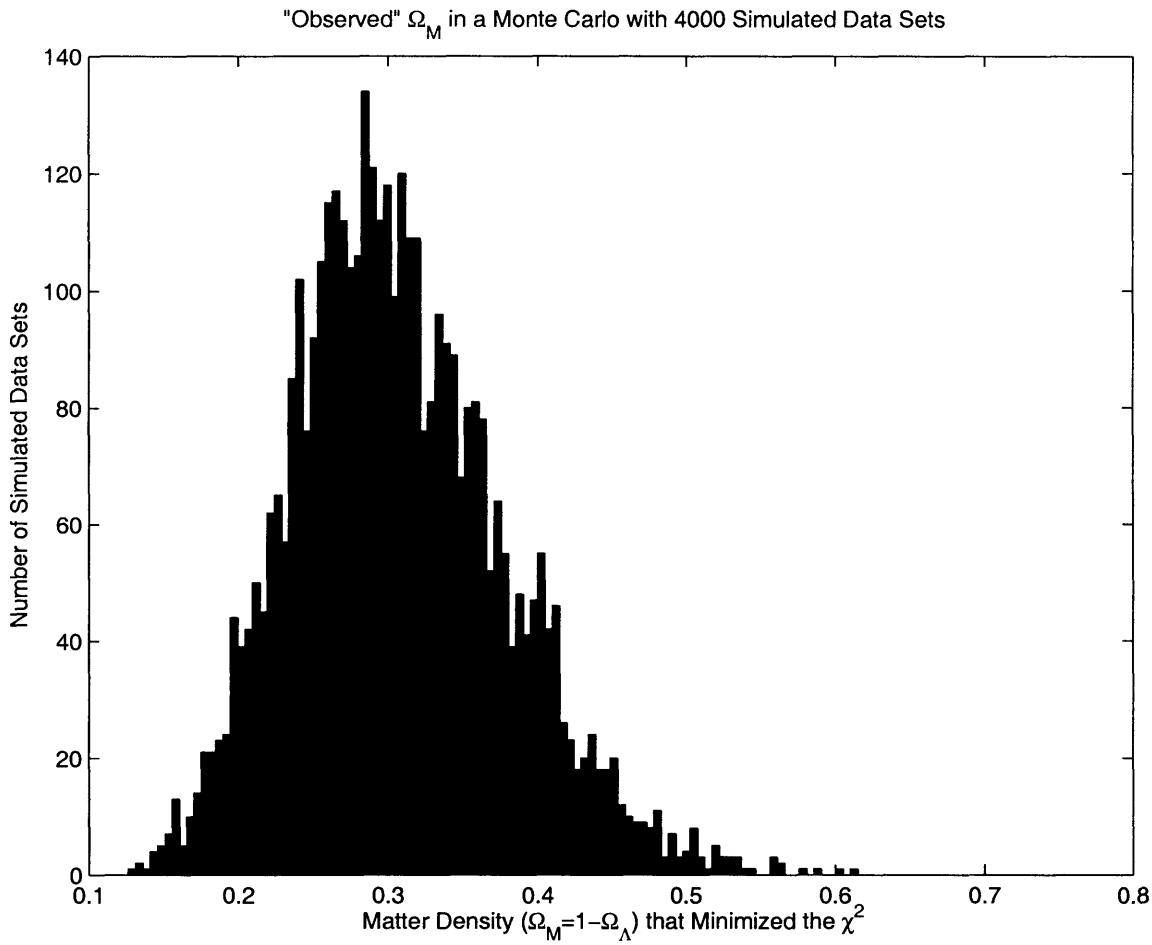

Figure 3-1: Monte Carlo results for 4000 simulated data sets, using the assumptions and procedure outlined in this chapter. This histogram shows the values of Ω_M that minimized each data set's χ^2 with $\Omega_M + \Omega - \Lambda = 1$ and $w = -1$.

unlike the others in this algorithm, directly corresponds to analysis that we would do on real data.

4. Repeat this process for thousands of simulated data sets to produce distributions of Ω_M, Ω_Λ, and w. The width of these distributions corresponds to the random error introduced by measurement uncertainties and propagated through to the measured cosmological parameters.

Appendix A contains the C code that implements this algorithm. Figure 3-1 shows the results of this simulation. The mean observed value of Ω_M in the simulation was 0.307 and the square root of the variance (which roughly corresponds to the error)

was 0.071. These results show a much smaller error than that predicted by the angular diameter distance ratio alone. This difference is due to the number of lenses in our sample. The distance ratio only takes one lens system into account while the Monte Carlo simulation made use of 19 lens systems. We expect the error in a fitted parameter to decrease as the square root of the sample size minus one. The error from the Monte Carlo sample is exactly that predicted error; the error associated with a single lens system (0.3) divided by the square root of the number of lens systems minus one ($\sqrt{18}$) gives the error generated in the Monte Carlo simulation (0.07). An even larger sample would give an even smaller error.

If the models of the universe and of gravitational lenses used in this simulation were accurate, we could expect to be able to constrain Ω_M to an error of better than 0.1 using only previously measured lens systems with known source redshifts and either four images or an Einstein ring. A measurement of Ω_M with an error of less than 0.1 is probably worth while, and with more lenses it is likely that the error could be further reduced. However, we know our model of lensing is overly simplistic. It is interesting, then, to examine the effect lens asymmetry has on the error of this measurement.

Chapter 4

Axisymmetric Lenses

Although a typical lensing galaxy likely has a triaxial ellipsoidal mass distribution [4], it is useful to introduce a model with an axisymmetric lens galaxy as a first test of our proposed measurements in the absence of spherical symmetry. There are two general categories of axisymmetric galaxies: oblate ellipsoids have two equal axes and one shorter axis, while prolate ellipsoids have two equal axes and one longer axis. We will proceed by separately examining the effect that each type of galaxy has on our predicted errors, then combining the two effects.

4.1 Modification of Equations for Prolate and Oblate Lenses

We construct a model for a singular isothermal ellipse (SIE) in parallel with our SIS model. The two dimensional projected mass profile of an SIS lensing galaxy is given by $\Sigma = \frac{\sigma_{v,SIS}^2}{2G}\frac{1}{r^2}$, where $\sigma_{v,SIS}$ is the line-of-sight velocity dispersion and r is the radial distance from the center. Kyu-Hyun Chae suggests that a corresponding formula for for an SIE lensing galaxy would be

$$\Sigma^{SIE} = \frac{\sigma_{v,SIE}^2}{2G}\frac{\sqrt{f}\lambda(q,f)}{\sqrt{x^2+f^2y^2}} \tag{4.1}$$

where $\sigma_{v,SIE}$ is the line-of-sight velocity dispersion of the SIE galaxy, $f = 1-\epsilon$ is the

ratio of the minor axis to the major axis of this projected distribution (also equal to one minus the ellipticity), q is the intrinsic axial ratio of the three dimensional mass distribution, and $\lambda(q, f)$ is a parameter introduced to characterize the dependence of $\sigma_{v,SIE}$ on the inclination angle and intrinsic shape of the galaxy. The factor $\lambda(q, f)$ affects the deflection angle and thus the image separation, in turn affecting the critical radius. Thus, additional uncertainty is introduced in our measurements through the parameter $\lambda(q, f)$, which is unknowable because q is indeterminable. In order to assess the severity of this additional error, we would like to find a probability distribution for λ in both oblate and prolate cases. We proceed by finding its dependence on q and f through extension of our SIE model. We will then generate a probability distribution based on the relationship between q and f.

The following analysis closely follows Kyu-Hyun Chae's derivations in his statistical analysis of the CLASS results [9], with some slight departures in order to obtain a model capable of dealing with individual lenses.

The density of an isothermal sphere is given by $\rho_{SIS} = \frac{\sigma_{v,SIS}^2}{2\pi G}\frac{1}{r^2}$ in spherical coordinates, where r is the distance radially from the center and $\sigma_{v,SIS}$ is the one-dimensional velocity dispersion. For this density distribution, isodensity contours are concentric spheres. In parallel, we construct a distribution with isodensity contours that are axisymmetric ellipsoids. This distribution, given in cylindrical coordinates (note that r has a different meaning than in the equation above), has $\rho_{SIE} = \frac{\sigma_{v,SIS}^2}{2\pi G}\frac{1}{r^2\left(\sin^2\theta + q^{-2}\cos^2\theta\right)}$, where q is the intrinsic axial ratio of the ellipsoid [9]. Oblate and prolate ellipsoids have $q < 1$ and $q > 1$, respectively. In this equation, $\sigma_{v,SIS}$ is a parameter that corresponds to the one dimensional velocity dispersion when $q = 1$. Throughout the rest of this paper, we define $q' \equiv |1 - q^2|^2$.

The one dimensional velocity dispersion of this galaxy will include contributions both from random thermal motion and from streaming motion of the particles in their orbits. The second velocity moments in the z direction (σ_z) and r direction (σ_r) can be calculated analytically, as well as the azimuthal component of the velocity distribution at any point, denoted σ_ϕ [9]. A Cartesian component σ_x^2 perpendicular to the axis of symmetry is given by $\sigma_x^2 = \sigma_r^2\cos^2\phi + \sigma_\phi^2\sin^2\phi$. Taking a mass-weighted

average gives greater weight to the components of the velocity dispersion where the density is greater. The mass-weighted average in units of $\sigma_{v,SIS}$ is given by

$$W = \frac{1}{\sigma_{v,SIS}^2 \int \rho \left(r^2 \sin\theta dr d\theta d\phi\right)} \int \rho\sigma^2 \left(r^2 \sin\theta dr d\theta d\phi\right). \tag{4.2}$$

For oblate ellipsoids, the mass-weighted averages of the x and z components are [9]:

$$W_x^{oblate}(q) = \frac{q}{q'} \arcsin q' \tag{4.3}$$

$$W_z^{oblate}(q) = \frac{1}{2}\frac{q}{q'}\left(\arctan\frac{q'}{q}\right)^{-1} \int_0^\pi d\theta \frac{1}{\sin\theta}\left(\arctan^2\frac{q'}{q} - \arctan^2\frac{q'\cos\theta}{q}\right) \tag{4.4}$$

For the prolate case, the corresponding equations are given by:

$$W_x^{prolate}(q) = \frac{1}{2}\frac{q}{q'} \ln\frac{q+q'}{q-q'} \tag{4.5}$$

$$W_z^{prolate} = \frac{1}{4}\frac{q}{q'}\left(\ln\frac{q+q'}{q-q'}\right)^{-1} \int_0^\pi d\theta \frac{1}{\sin\theta}\left[\left(\ln\frac{q+q'}{q-q'}\right)^2 - \left(\ln\frac{q+q'\cos\theta}{q-q'\cos\theta}\right)^2\right] \tag{4.6}$$

The line-of-sight velocity dispersion depends on the inclination of the galaxy, defined by the angle i between the unique axis and the observer. In terms of this angle and the above mass-weighted average second order velocity moments, the line-of-sight velocity dispersion is [9]

$$\sigma_{v,SIE}^2(i) = \sigma_{v,SIS}^2 \left[W_z(q)\cos^2 i + W_x(q)\sin^2 i\right]. \tag{4.7}$$

The above equation is true for both oblate and prolate lens galaxies.

Now that we have the velocity dispersions, we would like to relate this to the two dimensional projected mass distribution. These distributions are straightforward to calculate from our galaxy density distribution. They are given by [9]

$$\Sigma^{oblate} = \frac{\sigma^2_{v,SIS}}{2G} \frac{1}{\sqrt{x^2 + f^2 y^2}} \tag{4.8}$$

for oblate lenses and

$$\Sigma^{prolate} = \frac{\sigma^2_{v,SIS}}{2G} fq \frac{1}{\sqrt{x^2 + f^2 y^2}} \tag{4.9}$$

for prolate lenses. These projected mass distribution are characterized by f, the ratio of its minor axis to its major axis. For an oblate galaxy ($q < 1$), $f^2 = \cos^2 i + q^2 \sin^2 i = 1 = q'^2 \sin^2 i$, $i_{min} = \arcsin f'$ and $i_{max} = \frac{\pi}{2}$ corresponding to an edge-on view. For a prolate galaxy ($q > 1$), $f^2 = \left(\cos^2 i + q^2 \sin^2 i\right)^{-1} = \left(1 + q'^2 \sin^2 i\right)^{-1}$, $i_{min} = \arcsin\left(\frac{1}{sqrtq^2_{max}-1} \frac{f}{f'}\right)$, and $i_{max} = \frac{\pi}{2}$, where $q_{max} \approx 3.46717$ comes from the requirement that the second velocity moments be non-negative. f is measurable, in general, while q is not.

We compare these projected mass distributions to the mass distribution proposed at the beginning of the section and substitute in the formula for the line-of-sight velocity dispersion to obtain $\lambda(q, f)$. For oblate lensing galaxies, this gives

$$\lambda^{oblate}(q, f) = \frac{q}{\sqrt{f}} \frac{1}{W_z^{oblate} + \sin^2 i \left(W_x^{oblate} - W_z^{oblate}\right)}. \tag{4.10}$$

For prolate galaxies,

$$\lambda^{prolate}(q, f) = \frac{q\sqrt{f}}{W_z^{prolate} + f^2 \left(\frac{1-f^2}{q^2-1}\right) \left(W_x^{prolate} - W_z^{prolate}\right)} \tag{4.11}$$

4.2 Probability Density Function of $\lambda(q, f)$

Since galaxies are presumably oriented at random relative to us, each allowed inclination should be equally likely. Thus, for a given observed f with a galaxy assumed to be either oblate or prolate, i has a probability density function given by

$$P(i; f) = \begin{cases} \frac{1}{i_{max} - i_{min}(f)} & \text{for } i_{min}(f) < i < i_{max} \\ 0 & \text{otherwise} \end{cases}. \tag{4.12}$$

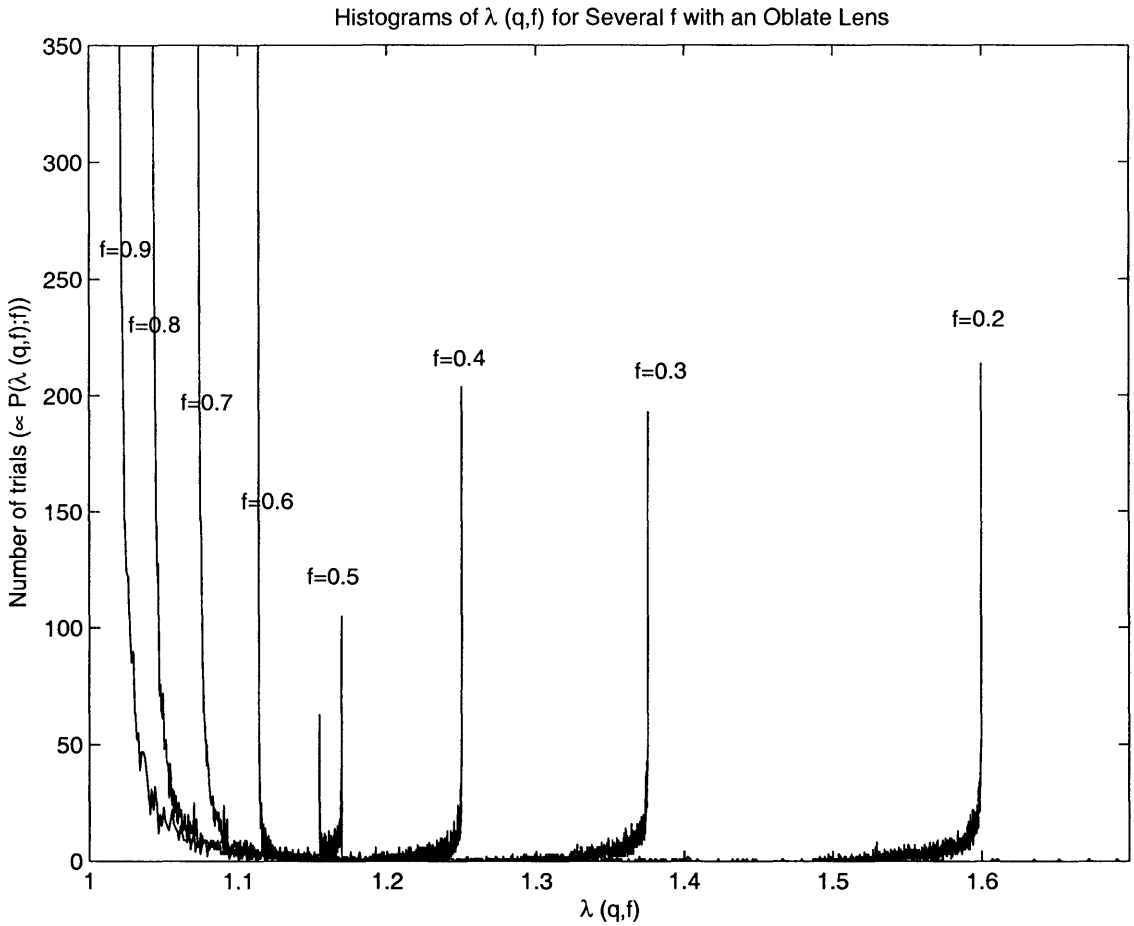

Figure 4-1: $P(\lambda(q,f);f)$ for several different values of f, assuming an oblate lensing galaxy. Sample size is 4000 for each distribution.

For each f, the probability density function associated with q can then be found by drawing many i's from $P(i;f)$ and calculating $q = \sqrt{\frac{f^2-cos^2 i}{sin^2 i}}$ for an oblate lens and $q = \sqrt{\frac{1-f^2\cos^2 i}{f^2\sin^2 i}}$ for a prolate one. Similarly, we calculate $P(\lambda(q,f);f)$ in both oblate and prolate cases by drawing random i's from $P(i;f)$, calculating the appropriate q, and using the appropriate equation for $\lambda(q,f)$ to generate many $\lambda(q,f)$'s.

We wrote a C program to do this particular calculation for both oblate and prolate cases, shown in Appendices B and C, respectively. Since f is measurable, we did not vary it within a calculation but rather calculated the probability distribution for many different f's in each case. The resulting probability density functions are show in Figures 4-1 and 4-2 and their means and standard deviations are shown in Tables 4.2 and 4.2. Although each probability distribution for a given lens model

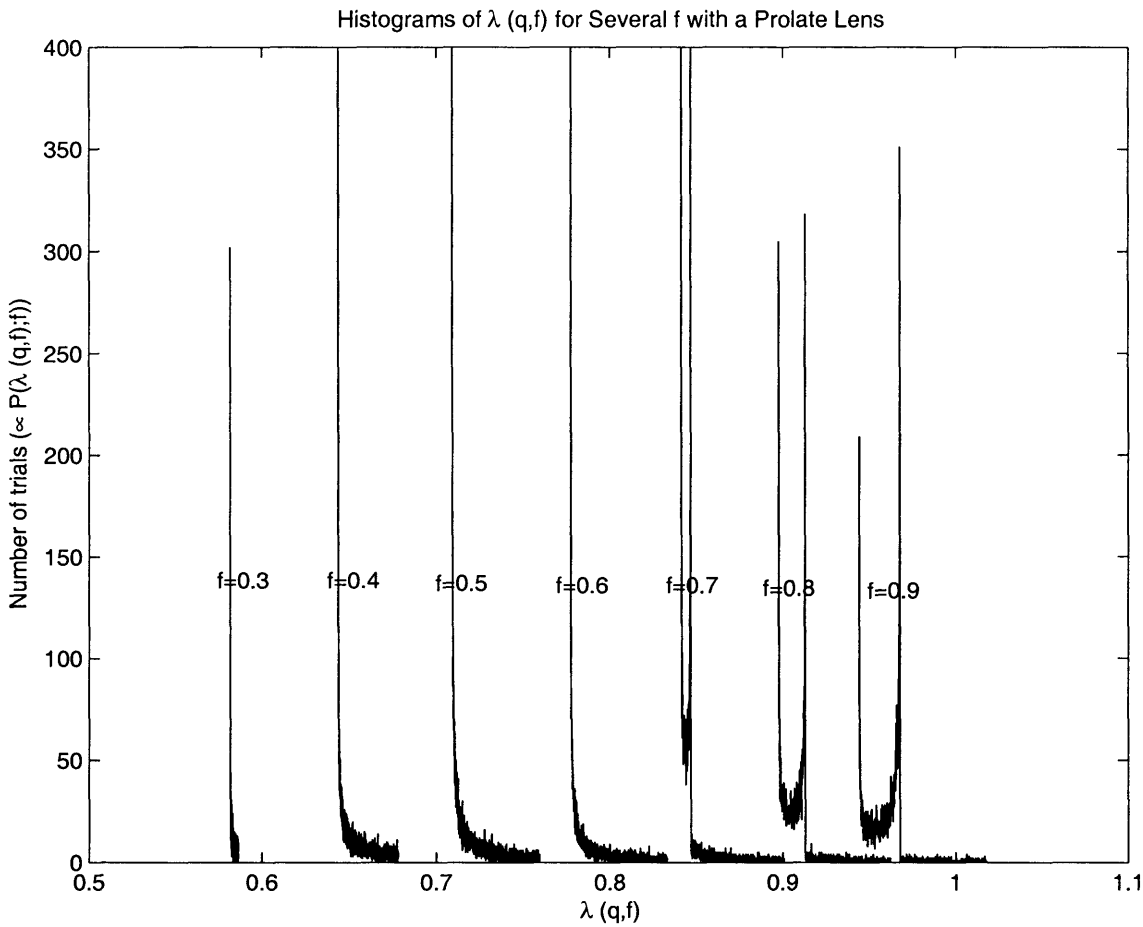

Figure 4-2: $P(\lambda(q, f); f)$ for several different values of f, assuming a prolate lensing galaxy. Sample size is 4000 for each distribution.

Table 4.1: The statistics of λ for known f and an oblate lens. For each f, we used 4000 simulated lens systems to generate these statistics.

f	Mean λ	Standard Deviation of λ
0.1	2.118	0.023
0.2	1.577	0.024
0.3	1.356	0.021
0.4	1.237	0.014
0.5	1.164	0.005
0.6	1.117	0.011
0.7	1.085	0.028
0.8	1.064	0.050
0.9	1.042	0.067

Table 4.2: The statistics of λ for known f and a prolate lens. For each f, we used 4000 simulated lens systems to generate these statistics.

f	Mean λ	Standard Deviation of λ
0.2	0.748	0.519
0.3	0.583	0.001
0.4	0.653	0.010
0.5	0.720	0.013
0.6	0.785	0.013
0.7	0.848	0.011
0.8	0.908	0.010
0.9	0.960	0.010

(oblate or prolate) and f has a small standard deviation, the difference between the oblate and prolate case is great for small f.

If we knew whether a galaxy was oblate or prolate, we could assume the mean value of λ for that f and obtain a small error from the standard deviation of the distribution of λ; however, we cannot determine the intrinsic shape of a galaxy. Assuming an axisymmetric lensing galaxy that may be either oblate or prolate, we cannot obtain a single value of λ that is most probable without knowing the inherent distribution of oblate and prolate galaxies. The best we can do is to assume λ=1 and increase our errors to compensate. The standard deviation of λ for a lens that may be either oblate or prolate is approximately half the difference of the means of the oblate and prolate distributions, a much larger error than that associated with either the oblate or prolate distribution alone. This error is only about ten percent, though, if we select lenses with $f > 0.8$ and it falls to five percent for $f > 0.9$. In practice, most real lens systems have $f > 0.8$, so our lens sample would only be slightly limited by such a selection.

Since $\lambda\sigma_v^2 \propto D_S/D_{LS}$, the uncertainty in λ for an axisymmetric lens effectively increases the uncertainty in σ_v^2 if that lens is treated as spherical. When two quantities with errors of ten percent (λ for $f > 0.8$ and σ_v^2) are multiplied together their product has an error of fourteen percent. A true prediction of the error in calculations of Ω_M made assuming spherical symmetry where galaxies are truly axisymmetric would require knowledge of the distribution of intrinsic galaxy shapes– the percentage that are

oblate versus prolate and the distribution of f. We do not at present have a reasonable model for such a distribution of intrinsic shapes. However, we may estimate the error introduced by the assumption of spherical symmetry by rerunning our Monte Carlo simulation from Chapter 3 with σ_v^2 errors of fourteen percent, increased from ten percent to mimic the effect of λ. In this simulation we obtained a mean best-fit Ω_M of 0.313 with a standard deviation of 0.10. If lenses were truly axisymmetric and we selected our lens sample with f's near enough to one, the error due to assuming spherical symmetry would be minimal, raising the error on Ω_M from 0.07 to 0.10.

Chapter 5

Conclusions

We assessed the feasibility of a technique for measuring Ω_M that makes use of gravitational lens geometry and velocity dispersions of lensing galaxies through the equation

$$\theta_E = 4\pi \frac{\sigma_v^2}{c^2} \frac{D_{LS}}{D_S}. \tag{5.1}$$

This equation assumes spherical symmetry in the lensing galaxy, something that we clearly cannot expect from real galaxies. Thus, it is important to assess both the error from imprecise measurements, dominated by σ_v, and the error produced by assuming spherically symmetric lenses when this is not truly the case. Our Monte Carlo simulation, which assumed that lenses truly are spherically symmetric, the universe is flat, and $\Omega_M = 0.3$, predicted an error of 0.07 for Ω_M.

We refined our lens model to an axisymmetric model using a multiplicative factor of λ in front of the velocity dispersion. We then generated probability distributions for this factor for various two dimensional mass profiles for both oblate and prolate galaxies. We found that for a given f with a galaxy known to be either oblate or prolate, λ had a very small standard deviation. However, oblate and prolate distributions diverged for small f. For $f > 0.8$, λ had a standard deviation of less than ten percent, leading to predicted error of 0.10 in Ω_M if galaxies are truly axisymmetric and we assume they are spherical in our analysis. Based on this analysis, this technique should produce measurements with usefully small errors, particularly

if a greater number of lenses are included in the sample. Although initial plots of the angular diameter distance ratio suggest that this technique is insufficiently sensitive to changes in w to measure it, it would be useful to do a similar analysis to the one we have done with w varied when minimizing the χ^2. This technique might also provide a measurement of w with a sufficiently large lens sample, a question left open by our analysis.

This analysis, however suggestive, is not sufficient in its own right to determine the feasibility of this technique. Galaxies are not truly spherical or axisymmetric, but rather triaxial. It should be possible, in principle, to adapt the technique we used for axisymmetric galaxies. Rather than a single uniformly distributed inclination angle, there would be two angles that each had equal probability of pointing in any direction but that had to be at 90 degrees to each other– the inclination angle of the longest axis and of the shortest axis. We could use these angles to relate intrinsic shape to projected mass distributions and through that to lensing geometry. The difficult part would be obtaining equations for the velocity dispersions. There is no known analytical solution for the velocity dispersion of such a galaxy. It is possible that Monte Carlo techniques could be used to obtain the velocity dispersion, as well, with the application of more detailed models of galactic dynamics. Such an analysis would be important to obtaining an estimate of the error associated with assuming spherical symmetry in the analysis of data taken on realistic galaxies.

Although we do not have a thorough analysis of the error introduced by assuming that galaxies are axisymmetric rather than triaxial, we can use oblate and prolate galaxies to bound the distribution. These types of galaxies represent the extreme cases of triaxial galaxies, where the middle axis is equal to the longest axis or the shortest axis. We would expect the probability distribution of λ for a triaxial galaxy to cover the space between the prolate and oblate distributions for the same f. Thus, for a given f, we can assume that the standard deviation of λ for triaxial galaxies will be equal to or smaller than that determined for axisymmetric galaxies. Although a simulation with triaxial galaxies would be necessary to obtain a real estimate of the error associated with this technique, our analysis with axisymmetric galaxies is

good enough to show that this technique has promise as a way to measure the matter density of the universe.

Appendix A

SIS Monte Carlo Code

Many of the functions used in the following code can be found in *Numerical Recipes in C.*[35]

```
/* mytrapzd and myqromb are alterations of Numerical Recipes */
/* functions.*/

#include <stdio.h>
#include <math.h>
#include <stdlib.h>
#define _XOPEN_SOURCE
#include <sys/time.h>
#undef _XOPEN_SOURCE
#include <float.h>

#define NRANSI
#include "nr.h"
#include "nrutil.h"

#define NUMLENSES 19
```

```
#define NUMSIMS 4000
#define SIGMAVERROR 0.05

float constant = 299792.458*299792.458/2.0/60.0/60.0/360.0;
  /* units are km^2/(s^2). const= (c^2/4/pi)*(1 arcmin/60 arcsec)*(1 degree/60 arcm

float epsilon = 0.01;
/* step size for evaluation of chi squareds */

/* File format: Inputs (objectname tab zsource tab zlens tab critrad)*/
/* Outputs (objectname tab zsource tab zlens tab critrad tab */
/* predicted_sigmav tab fake_observed_sigmav) */

/* This program generates many sample sets of observed one dimensional */
/* velocity dispersions of gravitational lens systems based */
/*  upon a real data set of zsource, zlens, and critrad. It uses    */
/* the equation: critrad = 4*pi*sigmav^2/c^2*(d_ls/d_os) where       */
/* d_ls is the angular diameter distance from the lens to the source */
/* and d_os is the angular diameter distance from the observer to    */
/* the source. sigmav is the velocity dispersion.  critrad is the */
/* critical radius                  */

/* To generate these sample sets, it is assumed that current observational */
/* errors have a gaussian distribution with a standard deviation of */
/* 5% of the measured velocity dispersion for each lens.           */

/* It is assumed that OmegaM = 0.3, OmegaLambda = 0.7. These values */
/* are necessary to calculate d_os and d_ls from zsource and zlens. */
/* OmegaRadiation is set to 0 (which is a decent approximation) and */
/* it is assumed that there is a cosmological constant (w=-1) */
```

```
/* This program will read in from a file containing three columns: */
/* zsource, zlens, and critrad. */


main()
{

  float d_ls;       /* distance from lens to source     */
  float d_os;       /* distance from observer to source */
  float zsource;    /* source redshift                  */
  float zlens;      /* lens redshift                    */
  float critrad;     /*Critical radius in arcseconds     */
  float sigmav;     /* predicted velocity dispersion    */
  float fakesigmav; /* fake observed sigmav (sigmav +error) */
  float error;
  float angdist(float,float,float,float,float,float);
  double radicand;
  char filein[15];  /* filename of input file             */
  char fileout[15];
  float sigmavs[NUMLENSES];
  float outputs[NUMLENSES][NUMSIMS];
  FILE *fopen(), *fpin, *fpout;
  float omegam=0.3;
  float lambda=0.7;
  float zl[NUMLENSES], zs[NUMLENSES],critrads[NUMLENSES];
  float omegaradiation=0.0;
  float w=-1.0;
  float chisquared,chisquaredplus,chisquaredminus, predsigmav;
  time_t sc;             /* time returned by system clock          */
```

```
long idum; /* seed for random number generator */
char objectname[50]; /* Name of the current gravitational lens system */
int lens, simnum=0, i, j;
float calculate_chi_squared(float zl[NUMLENSES],float zs[NUMLENSES],float critrad


/*prompt for input file name. prompt for output filename */
printf("Name of input file: ");
for (i = 0; (filein[i] = getchar()) != '\n'; ++i)
  ;
for (i; i<14;++i)
   filein[i]=0;
fpin = fopen(filein, "r");
printf("Name of output file: ");
for (i = 0; (fileout[i] = getchar()) != '\n'; ++i)
  ;
for (i; i<14;++i)
  fileout[i]=0;
fpout = fopen(fileout, "w");


/* seed random number generator with the clock */
sc = time(0);
idum = sc % 32766;
idum = (-1) * idum;


/* This loop creates a fake data set*/
lens=0;
while(fscanf(fpin,"%s\t%f\t%f\t%f\n",objectname,&zsource,&zlens,&critrad) != EOF)
```

```
  /*reads zsource, zlens, critrad in and tests for end of file*/
  /* calculate value of sigmav to output */
  d_os = angdist(0.0,zsource,omegam,lambda,omegaradiation,w);
  d_ls = angdist(zlens,zsource,omegam,lambda,omegaradiation,w);

  radicand = critrad*constant*d_os/d_ls;
  sigmav = sqrt(radicand);
  sigmavs[lens]=sigmav;

  zl[lens]=zlens;
  zs[lens]=zsource;
  critrads[lens]=critrad;

  /* generate error */
  for(simnum=0;simnum<NUMSIMS;simnum++){
    error = sigmav * SIGMAVERROR * gasdev(&idum);

    /* that generates errors with a gaussian distribution with */
    /* sigma=5% of sigmav, which simulates current errors in */
    /* observations */

    fakesigmav = sigmav+error;

    /* outputs */
    /* store the fake data in a huge array */
    outputs[lens][simnum]=fakesigmav;
  }
  lens++;
}
```

```
  /* this loop finds a local minimum in the chi squared */
  for(simnum=0;simnum<NUMSIMS;simnum++){

    /*initialize storage for chisquared evaluated at three test
      locations about a point, separated by epsilon */
    chisquaredplus=0.0;
    chisquaredminus=0.0;
    chisquared = 0.0;
    omegam=0.3;
    lambda=0.7;

    do{
      if(chisquared==0.0){
chisquared=calculate_chi_squared(zl,zs,critrads,outputs,sigmavs,omegam,lambda,omega
      }
      if(chisquaredplus==0.0){
chisquaredplus = calculate_chi_squared(zl,zs,critrads,outputs,sigmavs,omegam+epsilo
      }
      if(chisquaredminus==0.0){
chisquaredminus = calculate_chi_squared(zl,zs,critrads,outputs,sigmavs,omegam-epsil
      }

      if((chisquaredplus>chisquared)&&(chisquaredminus<chisquared)){
omegam=omegam-epsilon;
lambda=lambda+epsilon;
chisquaredplus=chisquared;
chisquared=chisquaredminus;
chisquaredminus=0;
      }else if((chisquaredplus<chisquared)&&(chisquaredminus>chisquared)){
omegam=omegam+epsilon;
```

```
lambda=lambda-epsilon;
chisquaredminus=chisquared;
chisquared=chisquaredplus;
chisquaredplus=0;
      }

    }while(!((chisquaredminus>chisquared)&&(chisquaredplus>chisquared)));

    printf("%d %f %f %f %f\n",simnum,omegam, lambda, w, chisquared);
    fprintf(fpout,"%f %f %f %f\n",omegam, lambda, w, chisquared);

  }
  fclose(fpin);
  fclose(fpout);
}


float calculate_chi_squared(float zl[NUMLENSES],float zs[NUMLENSES],float critrads[
{
  float radicand, predsigmav, d_os, d_ls, angdist(float,float,float,float,float,flo
  int lens;
  float chisquared=0.0;
  for(lens=0;lens<NUMLENSES;lens++){
    d_os = angdist(0.0,zs[lens],omega,lambda,radiation,w);
    d_ls = angdist(zl[lens],zs[lens],omega,lambda,radiation,w);
    radicand = critrads[lens]*constant*d_os/d_ls;
    predsigmav = sqrt(radicand);
    chisquared=chisquared+(outputs[lens][simnum]-predsigmav) * (outputs[lens][simnu
  }
  return chisquared;
```

```
}

float eqn(float x, float omega, float lambda, float radiation,float w)
{
  float k,n;
  n = 3.*(1.+w);
  k= 1-omega-lambda-radiation;

  return 1.0/sqrt(radiation*(1.+x)*(1.+x)*(1.+x)*(1.+x)
    + omega*(1.+x)*(1.+x)*(1.+x)
    + k*(1.+x)*(1.+x)
    + lambda*pow((1.+x),n));
}


float angdist(float z1,float z2,float omega,float lambda,float radiation,float w)

    /* Calculates the angular diameter distance between two redshifts    */
    /*   allowing lambda != 0, radiation pressure != 0, and other        */
    /*   models of dark energy.  Units are                               */
    /*   Mpc/h.                                                          */

    /*    z1 = first redshift                                            */
    /*    z2 = second redshift                                           */
    /*    omega = present value of matter density                        */
    /*    lambda = present value of scaled cosmological constant         */
    /*    radiation = present value of radiation density                 */
    /*    w = ratio of pressure over density                             */

    /* Formulae are those given by D. W. Hogg   astro-ph/9905116         */
```

```
    /*      and Kujat, Linn, Scherrer, and Weinberg   astro-ph/0112221   */
{
  float myqromb(float (*func)(float,float,float,float,float),float,float,float,floa
  float distance = 0 ;     /* value returned                        */
  float d_lc1 = 0;         /* line-of-sight comoving distance       */
  float d_lc2 = 0;
  float d_tc1 = 0;         /* transverse comoving distance          */
  float d_tc2 = 0;
  int nrecs = 1000;        /* number of rectangles for integration */
  float tolerance = 1;     /* tolerance for integration             */
  float old = 0;           /* stores integration result             */
  float z;
  float dz;                /* step size in integration              */
  float n;                 /* power of dark energy in E(z)          */
  float k;                 /* curvature density (omega_k)           */

  double d1, d2;

  n = 3.*(1.+w);
  k = 1.0-omega-lambda-radiation;

  /* numerically integrate to get line-of-sight comoving distances */
  d_lc1=myqromb(eqn,0.0,z1,omega,lambda,radiation,w);
  d_lc2=myqromb(eqn,0.0,z2,omega,lambda,radiation,w);

  /* transverse comoving distances; formula depends on curvature */
  if (fabs(k)<=10*FLT_EPSILON){
    /* flat */
    d_tc1 = d_lc1;
    d_tc2 = d_lc2;
```

```
  }else if (k < 0.0){
    /* positively curved */
    printf("Positive\n");
    d_tc1 = sinh((double) d_lc1 * sqrt(k)) / sqrt(k);
    d_tc2 = sinh((double) d_lc2 * sqrt(k)) / sqrt(k);
  }else{
    /* negatively curved */
    printf("Negative %f\n",k);
    d_tc1 = sin((double) d_lc1 * sqrt(k)) / sqrt(k);
    d_tc2 = sin((double) d_lc2 * sqrt(k)) / sqrt(k);
  }

  /* angular diameter distance from transverse comoving distance*/
  d1 = 1. + k * d_tc1 * d_tc1;
  d2 = 1. + k * d_tc2 * d_tc2;
  distance = (d_tc2 * sqrt(d1) - d_tc1 * sqrt(d2)) / (1.+z2);
  distance = 3000. * distance;

  return distance;

}

#define EPS 1.0e-6
#define JMAX 20
#define JMAXP (JMAX+1)
#define K 5

/* This is a modified Numerical Recipes function */

float myqromb(float (*func)(float,float,float,float,float), float a, float b,float
```

```
{
  void polint(float xa[], float ya[], int n, float x, float *y, float *dy);
  float mytrapzd(float (*func)(float,float,float,float,float), float a, float b, in
  void nrerror(char error_text[]);
  float ss,dss;
  float s[JMAXP],h[JMAXP+1];
  int j;

  h[1]=1.0;
  for (j=1;j<=JMAX;j++) {
    s[j]=mytrapzd(func,a,b,j,omega,lambda,radiation,w);
    if (j >= K) {
      polint(&h[j-K],&s[j-K],K,0.0,&ss,&dss);
      if (fabs(dss) <= EPS*fabs(ss)) return ss;
    }
    h[j+1]=0.25*h[j];
  }
  nrerror("Too many steps in routine qromb");
  return 0.0;
}
#undef EPS
#undef JMAX
#undef JMAXP
#undef K

/* This is a modified Numerical Recipes function. */

float mytrapzd(float (*func)(float,float,float,float,float), float a, float b, int
{
  float x,tnm,sum,del;
```

```
  static float s;
  int it,j;

  if (n == 1) {
    return (s=0.5*(b-a)*((*func)(a,omega,lambda,radiation,w)+(*func)(b,omega,lambda
  } else {
    for (it=1,j=1;j<n-1;j++) it <<= 1;
    tnm=it;
    del=(b-a)/tnm;
    x=a+0.5*del;
    for (sum=0.0,j=1;j<=it;j++,x+=del) sum += (*func)(x,omega,lambda,radiation,w);
    s=0.5*(s+(b-a)*sum/tnm);
    return s;
  }
}
```

Appendix B

Generating $P(\lambda(q, f); f)$ for Oblate Lenses

Many of the functions used in the following code can be found in *Numerical Recipes in C*.[35]

```
/* #include <stdio.h>
#include <stdlib.h> */
#include <math.h>
#define _XOPEN_SOURCE /* so sys/time.h won't include sys/select.h on solaris */
#include <sys/time.h>
#undef _XOPEN_SOURCE

#define NRANSI
#include "nrutil.h"
#include "nr.h"

float q_global, qp_global;
```

```
float eqn(float x)
{

  return  (atan(qp_global/q_global)*atan(qp_global/q_global)
   -atan(qp_global/q_global*cos(x))
   *atan(qp_global/q_global*cos(x)))/sin(x);

}




main()
{
  float f=0.9; /* 1-eccentricity of lensing galaxy 2-D profile */
  time_t sc;              /* time returned by system clock          */
  long idum; /* seed for random number generator */
  float i; /* inclination */
  float stuff;
  float wx;
  float wz;
  float lambda;
  FILE *fopen(), *fpout;
  int j;
  char fileout[15];
  float imin;
  float temp;
```

```
fpout=fopen("poflambda.txt","w");


/* seed random number generator with the clock */
sc = time(0);
idum = sc % 32766;
idum = (-1) * idum;


imin=asin(sqrt(1-f*f));

for(j=1;j<=4000;j++){
  i=(3.14159/2-imin)*ran1(&idum)+imin;
  /*printf("%f\n",cos(i));*/

  q_global=sqrt((f*f-cos(i)*cos(i))/sin(i)/sin(i));
  qp_global=sqrt(1-q_global*q_global);
  printf("q %f\n",q_global);

  wx=q_global/qp_global*asin(qp_global);
  stuff=qromo(eqn, 0.0, 3.14159,midpnt);
  wz=q_global/qp_global/2/(atan(qp_global/q_global))*stuff;


  lambda=q_global/sqrt(f)/(wz+(f*f-1)/(q_global*q_global-1)*(wx-wz));

  printf("lambda %f\n",lambda);
  fprintf(fpout,"%f %f %f\n",i,q_global,lambda);
}
fclose(fpout);}
```

Appendix C

Generating $P(\lambda(q, f); f)$ for Prolate Lenses

Many of the functions used in the following code can be found in *Numerical Recipes in C*.[35]

```
/* #include <stdio.h>
#include <stdlib.h> */
#include <math.h>
#define _XOPEN_SOURCE /* so sys/time.h won't include sys/select.h on solaris */
#include <sys/time.h>
#undef _XOPEN_SOURCE

#define NRANSI
#include "nrutil.h"
#include "nr.h"

float q_global, qp_global;
```

```
float eqn(float x)
{

  return ((log((q_global+qp_global)/(q_global-qp_global)))
  *(log((q_global+qp_global)/(q_global-qp_global)))
  -(log((q_global+qp_global*cos(x))/(q_global-qp_global*cos(x))))
  *(log((q_global+qp_global*cos(x))/(q_global-qp_global*cos(x))))
    /sin(x);
}

main()
{
  float f=0.9; /* 1-eccentricity of lensing galaxy 2-D profile */
  time_t sc;              /* time returned by system clock          */
  long idum; /* seed for random number generator */
  float i; /* inclination */
  float stuff;
  float wx;
  float wz;
  float qmax=3.46717;
  float lambda;
  FILE *fopen(), *fpout;
  int j;
  char fileout[15];
  float imin;
  float temp;



  fpout=fopen("poflambda.txt","w");
```

```
/* seed random number generator with the clock */
sc = time(0);
idum = sc % 32766;
idum = (-1) * idum;


imin=asin(sqrt(1-f*f)/f/sqrt(qmax*qmax-1));

for(j=1;j<=10000;j++){
  i=(3.14159/2-imin)*ran1(&idum)+imin;
  /*printf("%f\n",cos(i));*/
  q_global=sqrt((1-f*f*cos(i)*cos(i))/f/f/sin(i)/sin(i));
  qp_global=sqrt(q_global*q_global-1);
  /*printf("q %f\n",q_global);*/

  wx=q_global/qp_global/2*log((qp_global+q_global)/(q_global-qp_global));
  stuff=qromo(eqn, 0.0, 3.14159,midpnt);
  wz=q_global/qp_global/4/log((q_global+qp_global)/(q_global-qp_global))*stuff;


  lambda=q_global*sqrt(f)/(wz+f*f*(1-f*f)/(q_global*q_global-1)*(wx-wz));

  /*    printf("lambda %f\n",lambda);*/
  fprintf(fpout,"%f %f %f\n",i,q_global,lambda);
}

fclose(fpout);}
```

Bibliography

[1] R. W. Porcas M. A. Garrett A. R. Patnaik, A. J. Kemball. Milliarcsec-scale polarization observations of the gravitational lens b1422+231. *Monthly Notices of the Royal Astronomical Society*, 307(1), July 1999.

[2] Ramesh Narayan & Matthais Bartelmann. Lectures on gravitational lensing. Archived at http://lanl.arxiv.org/abs/astro-ph/9606001, June 1996. Lectures given at 13th Jerusalem Winter School in Theoretical Physics: Formation of Structure in the Universe, Jerusalem, Israel, 27 Dec 1995- 5 Jan 1996.

[3] Danielle; Guilloteau Stephane; Antonucci Robert Barvainis, Richard; Alloin. Detection of co (3–2) emission at z = 2.64 from the gravitationally lensed quasar mg 0414+0534. *Astrophysical Journal Letters*, 492, January 1998.

[4] James Binney and Scott Tremaine. *Galactic Dynamics.* Princeton University Press, 1987.

[5] A. R.; Walsh D.; Wilkinson P. N. Browne, I. W. A.; Patnaik. The redshift of the lensing galaxy in the gravitationally lensed system b:0218+35.7. *R.A.S. Monthly Notices (MNRAS)*, 263(3), August 1993.

[6] I.; et. al. Burud. High-resolution optical and near-infrared imaging of the quadruple quasar rx j0911.4+0551. *Astrophysical Journal Letters*, 501, July 1998.

[7] Sean M. Carroll. *An Introduction to General Relativity Spacetime and Geometry.* Addison-Wesley, 2004.

[8] K.H. Chae and D. A. Turnshek. Hubble space telescope observations of the gravitationally lensed cloverleaf broad absorption line qso h1413+1143: modeling the lens. *The Astrophysical Journal*, 514(2):587–597, April 199.

[9] Kyu-Hyun Chae. The cosmic lens all-sky survey: statistical strong lensing, cosmological parameters, and global properties of galaxy populations. *Monthly Notices of the Royal Astronomical Society (MNRAS)*, 346(3):746–772, December 2003.

[10] O.; Hammer F.; Lilly S. J. Crampton, D.; Le Fevre. The gravitational lens cfrs14.1311 = hst 14176+5226. *Astronomy and Astrophysics*, 307:L53–L56, March 1996.

[11] C. Impey J. Lehar B. McLeod H.-W. Rix C.S. Kochanek, E.E. Falco. Castles survey. http://cfa-www.harvard.edu/castles/, 2002.

[12] Joseph; Shapiro Irwin I. Falco, Emilio E.; Lehar. Hst observations and models of the gravitational lens system mg 0414+0534. *Astronomical Journal*, 113:540, February 1997.

[13] C. D; et. al. Fassnacht. 1608+656: A gravitationally lensed poststarburst radio galaxy. *Astrophysical Journal Letters*, 460, April 1996.

[14] Judith G. Fassnacht, Christopher D.; Cohen. Keck spectroscopy of three gravitational lens systems discovered in the jvas and class surveys. *Astronomical Journal*, 115:377, February 1998.

[15] William J.; Broadhurst Tom Frye, Brenda; Welch. Resolving redshifted molecular absorption toward the gravitational lens pks 1830-211. *Astrophysical Journal Letters*, 478, March 1997.

[16] James B. Hartle. *Gravity: An Introduction to Einstein's General Relativity.* Addison-Wesley, 2003.

[17] David W. Hogg. Distance measures in cosmology. astro-ph preprints archive: http://lanl.arxiv.org/abs/astro-ph/9905116, December 2002.

[18] P.; Browne I.; Fassnacht C.D.; Koopmans L.; Marlow-D. Wilkinson P.N. Jackson, N.; Helbig. Lensing galaxies: light or dark? *Journal of Astronomy and Astrophysics*, 334:L33–L36, June 1998.

[19] C. S. Keeton, C. R.; Kochanek. Determining the hubble constant from the gravitational lens pg 1115+080. *Astrophysical Journal*, 487:42, September 1997.

[20] Christopher S. Kochanek. Evidence for dark matter in mg 1654+134. *Astrophysical Journal*, 445(2):559–577, June 1995.

[21] P.; Bartelmann M. Kormann, R.; Schneider. A gravitational lens model for b 1422+231. *Astronomy and Astrophysics*, 286(2):357–364, June 1994.

[22] Judith G.; Blandford Roger D.; Lubin Lori M. Kundic, Tomislav; Cohen. Keck spectroscopy of the gravitational lens system pg 1115+080: Redshifts of the lensing galaxies. *Astronomical Journal*, 114:507–510, August 1997.

[23] G. I.; et. al. Langston. Mg 1654+1346 - an einstein ring image of a quasar radio lobe. *Astronomical Journal*, 97:1283–1290, May 1989.

[24] Richard; Januzzi B. T.; Turner E. L. Lawrence, C. R.; Elston. Mg 0414+0534: A dusty gravitational lens. *Astronomical Journal*, 110(110):2570, December 1995.

[25] C.; et. al. Lidman. The redshift of the gravitationally lensed radio source pks 1830-211. *The Astrophysical Journal*, 514(2):L57–L60, April 1999.

[26] C. D.; Readhead A. C. S.; Blandford-R. D.; Ku ndic T. Lubin, L. M.; Fassnacht. A keck survey of gravitational lens systems. i. spectroscopy of sbs 0909+ 532, hst 1411+5211, and class b2319+051. *Astronomical Journal*, 119(2):451–459, February 2000.

[27] Sunita Mathur, Smita; Nair. X-ray absorption toward the einstein ring source pks 1830-211. *Astrophysical Journal*, 484:140, July 1997.

[28] S. T.; et. al. Myers. 1608+656: A quadruple-lens system found in the class gravitational lens survey. *Astrophysical Journal Letters*, 447, July 1995.

[29] Stefi A.; Stanghellini Carlo; Dey Arjun; van Breugel Wil; Deustua Susana; Smith Eric P. O'Dea, Christopher P.; Baum. Radio and optical observations of 0218+357 - the smallest einstein ring? *Astronomical Journal (AJ)*, 104(4):1320–1330, October 1992.

[30] A. R.; et. al. Patnaik. B1422+231 - a new gravitationally lensed system at z = 3.62. *Royal Astronomical Society, Monthly Notices*, 259(1):1P–4P, November 1992.

[31] Eric J.; Griffiths Richard E.; Im Myu ngshin Ratnatunga, Kavan U.; Ostrander. New "einstein cross" gravitational lens candidates in hubble space telesc ope wfpc2 survey images. *Astrophysical Journal Letters*, 453, November 1995.

[32] H.-J.; Baade R.; Lopez S; Tytler D. Reimers, D.; Hagen. Discovery of a new quadruply lensed qso: Hs0810+2554– a brighter twin to pg 1115+080. *Astronomy & Astrophysics*, 382:L26–L28, 2002.

[33] Neta A. Bahcall; Jeremaiah P. Ostriker; Saul Perlmutter; Paul J. Steinhardt. The cosmic triangle: Revealing the state of the universe. *Science*, 284:1481, 1999.

[34] Edwin F. Taylor and John Archibald Wheeler. *Exploring Black Holes: Introduction to General Relativity.* Addison-Wesley-Longman, 2000.

[35] William H. Press; Saul A Teukolsky; and Brian P. Flannery. *Numerical Recipes in C: The Art of Scientific Computing.* Cambridge University Press, 1992.

[36] Christopher S. Tonry, John L.; Kochanek. Redshifts of the gravitational lenses mg 0414+0534 and mg 0751+2716. *The Astronomical Journal*, 117(5):2034–2038, May 1999.

[37] Christopher S. Tonry, John L.; Kochanek. Redshifts of the gravitational lenses mg 0414+0534 and mg 0751+2716. *Astronomical Journal*, 117(5):2034–2038, May 1999.

[38] A.; Hewett P. C.; Shaver P. A. Warren, S. J.; Iovino. Spectroscopy of the optical einstein ring 0047-2808. *Monthly Notices of the Royal Astronomical Society (MNRAS)*, 299(4):1215–1219, October 1998.

[39] P. C.; Lewis G. F.; Moller P.; Iovino A.; Shaver P. A. Warren, S. J.; Hewett. A candidate optical einstein ring. *Monthly Notices of the Royal Astronomical Society (MNRAS)*, 278(1), January 1996.

[40] & Combes F. Wiklind, T. Co, hco^+ and hcn absorption in the gravitational lens candidate b0218+357 at z =0.685. *Astronomy and Astrophysics (A&A)*, 299:382, July 1995.

[41] N.; Liu M. C.; Maza J.; Morgan N. D.; Schechter P. L. Wisotzki, L.; Christlieb. 1999. *Journal of Astronomy and Astrophysics*, 348:L41–L44, August 1999.

[42] R. S.; Gunn J. E.; Westphal J. A.; Kristian J. Young, P.; Deverill. The triple quasar q1115+080a, b, c - a quintuple gravitational lens image. *Astrophysical Journal*, 244:723–725, March 1981.